

Increased cerebrospinal fluid albumin and immunoglobulin A fractions forecast cortical atrophy and longitudinal functional deterioration in relapsing-remitting multiple sclerosis

Julia Kroth, Dumitru Ciolac, Vinzenz Fleischer, Nabin Koirala, Julia Krämer, Muthuraman Muthuraman, Felix Luessi, Stefan Bittner, Gabriel Gonzalez-Escamilla, Frauke Zipp, Sven G. Meuth and Sergiu Groppa

Abstract

Background: Currently, no unequivocal predictors of disease evolution exist in patients with multiple sclerosis (MS). Cortical atrophy measurements are, however, closely associated with cumulative disability.

Objective: Here, we aim to forecast longitudinal magnetic resonance imaging (MRI)-driven cortical atrophy and clinical disability from cerebrospinal fluid (CSF) markers.

Methods: We analyzed CSF fractions of albumin and immunoglobulins (Ig) A, G, and M and their CSF to serum quotients.

Results: Widespread atrophy was highly associated with increased baseline CSF concentrations and quotients of albumin and IgA. Patients with increased CSF_{IgA} and CSF_{IgM} showed higher functional disability at follow-up.

Conclusion: CSF markers of blood–brain barrier integrity and specific immune response forecast emerging gray matter pathology and disease progression in MS.

Keywords: Multiple sclerosis, cerebrospinal fluid albumin, cerebrospinal fluid immunoglobulins, cortical gray matter, atrophy rate

Introduction

Multiple sclerosis (MS) is a chronic neuroinflammatory disease of the central nervous system (CNS) that leads to progressive disability. Recent neuroimaging, immunological, and histopathological studies have provided valuable insights into the mechanisms of the disease.^{1,2} Development of novel biomarkers is, however, essential since they should serve as optimized predictors for the disease course. Cortical atrophy represents an important magnetic resonance imaging (MRI)-based biomarker that is closely associated with emerging clinical disability.³ However, there are currently no unequivocal non-invasive predictors of

ongoing neuroinflammation and damage in the cortex.

The blood–brain barrier (BBB) plays an important role in MS pathogenesis, being the selective gatekeeper for immunoinflammatory responses in the CNS and the target of present and future drug developments.⁴ Cellular and molecular immune system components can cross the pathologically permeable BBB and trigger distinct inflammatory activity in different CNS compartments. BBB disruption has been attested not only in acute lesions, but also in normal-appearing gray and white matter.^{5,6}

Correspondence to:

S Groppa

Department of Neurology,
Focus Program Translational
Neuroscience (FTN),
Research Center for
Immunology (FZI), Rhine-
Main Neuroscience Network
(rnn²), University Medical
Center of the Johannes
Gutenberg University Mainz,
Langenbeckstraße 1, Mainz
55131, Germany.
segroppa@uni-mainz.de

Julia Kroth

Vinzenz Fleischer

Nabin Koirala

Muthuraman Muthuraman

Felix Luessi

Stefan Bittner

Gabriel Gonzalez-Escamilla

Frauke Zipp

Sergiu Groppa

Department of Neurology,
Focus Program Translational
Neuroscience (FTN),
Research Center for
Immunology (FZI), Rhine-
Main Neuroscience Network
(rnn²), University Medical
Center of the Johannes
Gutenberg University Mainz,
Mainz, Germany

Dumitru Ciolac

Department of Neurology,
Focus Program Translational
Neuroscience (FTN),
Research Center for
Immunology (FZI), Rhine-
Main Neuroscience Network
(rnn²), University Medical
Center of the Johannes
Gutenberg University Mainz,
Mainz, Germany/Department
of Neurology, Institute
of Emergency Medicine,
Laboratory of Neurobiology
and Medical Genetics,
Nicolae Testemitanu State
University of Medicine
and Pharmacy, Chisinau,
Moldova

Under physiological conditions, only low amounts of albumin and certain immunoglobulin (Ig) types cross the BBB. Albumin quotient (i.e. cerebrospinal fluid (CSF) albumin/serum albumin ratio) can therefore be considered a marker of BBB permeability.^{7,8} Addressing BBB integrity and longitudinal gray matter processes could translate inflammatory activity to focal and global brain atrophy, the latter being an accepted biological hallmark of the clinical long-term outcome.

Here, we investigate the connection between cortical atrophy and the presence of CSF markers of BBB permeability/integrity. We observed a significant correlation between CSF albumin and IgA and the rate of cortical atrophy over 12 months. We propose that elevated baseline levels of CSF albumin and IgA can serve as markers of early cortical atrophy and rapid disease progression in MS.

Methods

Patients

Seventy-one relapsing-remitting multiple sclerosis (RRMS) patients (mean age \pm standard deviation (SD) 31.2 ± 9.4 years, 25 males) were included in this longitudinal study. RRMS diagnosis was established accordingly to the 2010 revised McDonald diagnostic criteria.⁹ All patients underwent comprehensive clinical, laboratory, and neuroimaging evaluation through a standardized protocol.¹⁰ All patients were rescanned with the same protocol after 12 ± 1 months. The sustained Expanded Disability Status Scale (EDSS) score (confirmed after 3 months) at the second time point has been used as a clinical outcome measure to quantify clinical disability. We opted to use an EDSS score of 2 as a cut-off, since an EDSS score of <2.0 with at least 10 years of disease duration seems to be the most appropriate criterion in identifying patients with benign MS (Glad et al., 2010). Clinical disease activity was defined as a clinical relapse, while radiological activity was defined as the appearance of new/enlarging hyperintense lesions or gadolinium-enhancing lesions. Of 71 patients, 63 patients (89%) were receiving different disease-modifying treatment (DMT) and 8 patients were not on DMT. Informed consent was obtained from all patients and the study was approved by the local ethics committee.

CSF variables examination

CSF and serum samples were obtained from each patient at the time of first clinical event and CSF concentrations of albumin (CSF_{Alb}), IgA (CSF_{IgA}), IgG (CSF_{IgG}), and IgM (CSF_{IgM}) were determined with

immunonephelometry. Quotients of albumin (Q_{Alb}), IgA (Q_{IgA}), IgG (Q_{IgG}), and IgM (Q_{IgM}) were defined as the ratios of CSF concentrations to the corresponding serum concentrations of these fractions; reference values were considered according to Berlit.¹¹ Since Q_{Alb} is age-sensitive, increased Q_{Alb} was considered in relation to reference ranges depending on the age of the patients: 6.5–8 for patients aged <40 years (55 patients) and ≥ 8.0 for patients aged ≥ 40 years (16 patients).¹² To detect patients with intrathecal synthesis of IgA, IgG, and IgM, hyperbolic functions for each Ig type were applied as follows

$$Ig_{loc} = Q(Ig) - a / b \sqrt{(Q_{Alb})^2 + b^2} + c$$

where Ig_{loc} is local Ig synthesis, $Q(Ig)$ is Ig quotient, Q_{Alb} is albumin quotient, and a , b , and c are empirical values.¹³

MRI acquisition

Structural MRI images were acquired using a 3T Magnetom Tim Trio scanner (Siemens Medical Solutions, Erlangen, Germany) with a 32-channel head coil, according to a standardized protocol¹⁰ at the Neuroimaging Centre (NIC) Mainz, Germany. This imaging protocol comprises sagittal three-dimensional T1- and T2-weighted fluid-attenuated inversion recovery (FLAIR) sequences. T1-weighted magnetization-prepared rapid gradient echo (MP-RAGE) sequence included the following acquisition parameters: repetition time (TR) = 1900 ms, echo time (TE) = 2.52 ms, inversion time (TI) = 900 ms, echo train length (ETL) = 1, flip angle = 9° , matrix size = 256×256 , field of view (FOV) = 256×256 mm, slice thickness = 1 mm, voxel size = $1 \times 1 \times 1$ mm; FLAIR sequence: TR = 5000 ms, TE = 388 ms, TI = 1800 ms, ETL = 848, matrix size = 256×256 , FOV = 256×256 mm, slice thickness = 1 mm, voxel size = $1 \times 1 \times 1$ mm. T1-weighted, T2-FLAIR, and contrast-enhanced T1 images were analyzed by an experienced neuroradiologist for the detection of new and contrast-enhancing lesions.

Initially, lesion maps were drawn on T2-weighted 3D FLAIR images using the MRICron software (<http://www.mccauslandcenter.sc.edu/mricron/mricron/>). Using the lesion segmentation toolbox (LST) which is part of the statistical parameter mapping (SPM8) software, 3D FLAIR images were co-registered to 3D T1 images and bias corrected. After partial volume estimation (PVE), lesion segmentation was performed with 20 different initial threshold values for the lesion growth algorithm.¹⁴ By comparing automatically and

Table 1. Baseline demographic, clinical, and CSF data of RRMS patients.

Parameter	Mean \pm SD	Reference range
Age (years)	31.2 \pm 9.4	
Male/female: number (%)	25 (35%)/46 (65%)	
Age at diagnosis (years)	30.7 \pm 9.6	
Disease duration (years)	1.5 \pm 3.4	
EDSS	1.5 \pm 1.4	
CSF albumin (CSF _{Alb})	234.1 \pm 123.7 mg/L	110–350 mg/L
CSF IgA (CSF _{IgA})	3.2 \pm 3.2 mg/L	1.5–6 mg/L
CSF IgG (CSF _{IgG})	58.0 \pm 36.8 mg/L	<40 mg/L
CSF IgM (CSF _{IgM})	1.1 \pm 1.8 mg/L	<1 mg/L
Albumin quotient (Q _{Alb})	5.3 \pm 2.7	\leq 6.5 (<40 years) \leq 8 (>40 years)
IgA quotient (Q _{IgA})	1.6 \pm 1.4	1.3
IgG quotient (Q _{IgG})	5.1 \pm 2.9	2.3
IgM quotient (Q _{IgM})	1.1 \pm 1.8	0.3

SD: standard deviation; EDSS: Expanded Disability Status Scale; CSF: cerebrospinal fluid; Ig: immunoglobulin; Q: quotient; Ig: immunoglobulin.

manually estimated lesion maps, the optimal threshold (κ value, dependent on image contrast) was determined for each patient and an average value for all patients was calculated. Afterward, for automatic lesion volume estimation and filling of 3D T1 images, a uniform κ value of 0.1 was applied for all patients. Subsequently, the filled 3D T1 images as well as the native 3D T1 images were segmented into gray matter, white matter, and CSF and normalized to Montreal Neurological Institute (MNI) space. Finally, the quality of the segmentations was visually inspected.

MRI data processing: cortical thickness reconstruction

T1-weighted images were analyzed using FreeSurfer software (v5.3.0, <http://surfer.nmr.mgh.harvard.edu/>) for longitudinal cortical thickness (CT) and thalamic volume estimation in a fully automated fashion. In brief, after individual surface reconstruction, an unbiased within-subject template was created.^{15,16} The unbiased template served for initialization of skull stripping, normalization, atlas registration, and parcellation of individual time points.¹⁷ Surface maps of regional atrophy rates were computed as $(\text{thickness}_2 - \text{thickness}_1)/(\text{time}_2 - \text{time}_1)$ and smoothed with a 10 mm full width at half maximum (FWHM) Gaussian kernel for further correlation with CSF variables and their quotients. Statistical maps of significant correlations were corrected for multiple comparisons using false discovery rate (FDR, $p < 0.05$) with a minimum cluster size of 100 mm².

Statistical analysis

SPSS 23.0 software (IBM, Armonk, NY, USA) was used to perform statistical analyses. The data were checked for normal distribution using the Shapiro–Wilk test. Summary statistics are presented as mean \pm SD, median, and percentage, where applicable. Standard and stepwise linear regression analyses were performed to assess the relative contributions of baseline quotients (Q_{Alb}, Q_{IgA}, Q_{IgG}, and Q_{IgM}) in predicting the rate of cortical atrophy at 1-year follow-up. Adjusted R^2 values are reported. One-sided paired student's t-test was used to evaluate the differences in variables. P -values less than 0.05 were considered statistically significant. To account for a possible influence on cortical atrophy rates, age and gender of the patients were included as covariates.

Results

Patients

Baseline characteristics of the patients are reported in Table 1. In 68 patients, the CSF was positive for oligoclonal bands (OCB); two patients were OCB negative. During the 1-year follow-up, 18 patients (25.4%) presented a clinical relapse, 22 (31.0%) had MRI activity, and 11 (15.5%) presented both; the remaining patients (28.1%) were clinically and radiologically stable. Two patients exhibited new cortical lesions (precuneus and frontal). At follow-up, mean CT (2.52 ± 0.1 mm) and thalamus volume (8954.9 ± 1255.7 mm³) were significantly smaller in comparison to baseline values (2.53

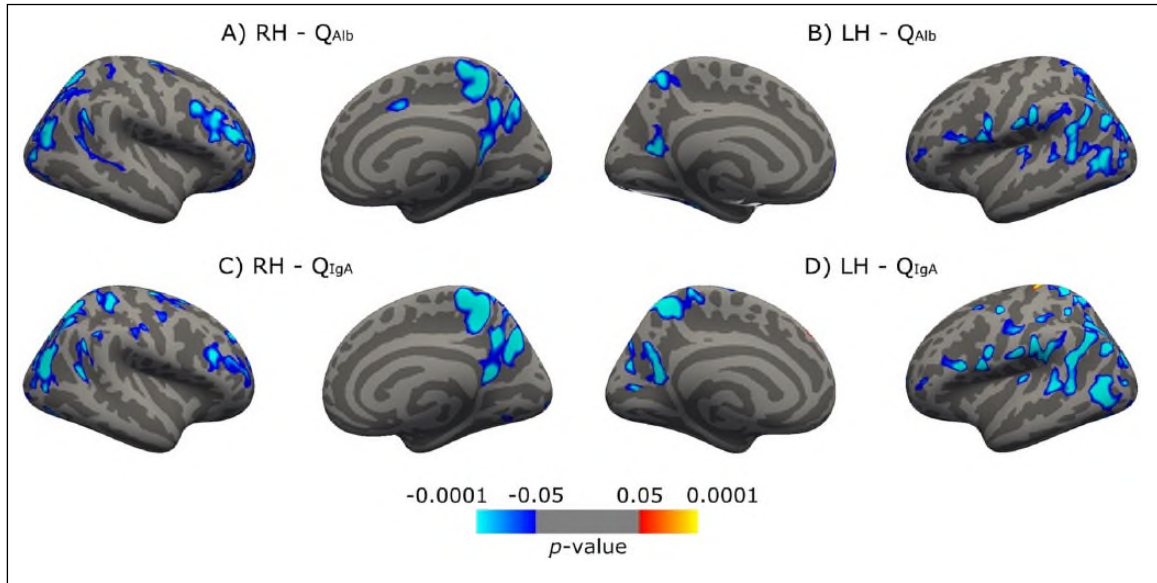


Figure 1. Clusters of significant associations between cortical atrophy rates and (A, B) albumin quotient (Q_{Alb}) and (C, D) IgA quotient (Q_{IgA}). Lateral and medial views of right (RH) and left (LH) hemispheres are shown. All labeled clusters were significant after FDR correction ($p < 0.05$). The color bar represents the statistical significance of the association.

± 0.1 mm, $p = 0.04$ and 9030.9 ± 1211.1 mm³, $p = 0.006$; respectively).

while Q_{IgM} correlated with the atrophy rate in the left parietal region.

Q_{Alb} , Q_{IgA} , and cortical atrophy rate

The rate of cortical atrophy over 1 year was highly associated with Q_{Alb} and Q_{IgA} . Significant correlations between atrophy rates and both baseline Q_{Alb} and baseline Q_{IgA} were found in the precuneus (PrC), rostral middle frontal (rMF), precentral (PC), and inferior parietal (IP) gyri of both hemispheres (Figure 1). Specific anatomic locations of these clusters are reported in Supplementary Table 1. The regions with the highest association between baseline Q_{Alb} and cortical atrophy rate were the right PrC ($R^2 = 0.364$, $p < 0.001$) and left fusiform gyrus ($R^2 = 0.290$, $p < 0.001$). Bilateral PrC had the highest associations with Q_{IgA} ($R^2 = 0.415$ for left and $R^2 = 0.503$ for right hemispheres, $p < 0.0001$).

Q_{Alb} , Q_{IgA} , and thalamic atrophy rate

No significant associations between the addressed quotients and the annual rate of thalamus atrophy were detected.

Q_{IgM} , Q_{IgG} , and cortical atrophy rate

Cortical atrophy rates were also associated with Q_{IgG} ($R^2 = 0.259$, $p = 0.02$, pars opercularis) and Q_{IgM} ($R^2 = 0.358$, $p = 0.04$, precentral cortex), although with a weaker effect size. Additional associations with Q_{IgG} were found in the right parietal and occipital lobes,

CSF fractions and cortical atrophy

Higher values of CSF_{Alb} and CSF_{IgA} were mirrored by increased regional gray matter loss. The annual rate of cortical atrophy correlated with CSF_{Alb} ($R^2 = 0.17$, $p < 0.001$, precuneus bilateral), CSF_{IgA} ($R^2 = 0.12$, $p = 0.001$), and to a lesser extent with CSF_{IgG} ($R^2 = 0.12$, $p = 0.02$) and CSF_{IgM} ($R^2 = 0.21$, $p = 0.04$) (Supplementary Figure 1).

CSF variables and EDSS

CSF_{IgA} and CSF_{IgM} significantly differed between patients with mild disability (EDSS 0–1.5) and those with an EDSS score between 2 and 6 at the second time point (IgA: 1.67 ± 0.69 mg/L vs 2.03 ± 0.71 mg/L, IgM: 9.87 ± 2.38 mg/L vs 11.5 ± 2.03 mg/L, $p = 0.04$ and $p = 0.003$, respectively). CSF_{Alb} , CSF_{IgG} , and the quotients showed no further correlations with the EDSS scores at the first or second time points.

Discussion

Identification of reliable early diagnostic immunological candidates that mirror ongoing disease activity and the long-term outcome in patients with MS is essential for therapeutic decisions in the era of rapidly increasing options for immune modulation. Here, we

identified increased CSF_{Alb} and CSF_{IgA} in patients with RRMS as early markers of cortical atrophy and emerging clinical disability. As these variables strongly reflect BBB integrity, we clearly demonstrate the link of ongoing inflammatory disease activity and cortical degeneration.

Histopathological analyses have confirmed the occurrence of BBB damage, inflammatory activity, and demyelination within the cortex in early MS patients, even preceding white matter lesions.¹⁸ Increased CSF_{Alb} and Q_{Alb} have been previously postulated to be indicators of BBB permeability.¹⁹ Our results show an association between CSF_{Alb}, Q_{Alb}, and cortical atrophy, and an even stronger effect for CSF_{IgA} and Q_{IgA}. Based on the topological similarity of cortical atrophy patterns for CSF_{Alb}, CSF_{IgA}, and their quotients, common mechanisms reflecting BBB disruption can be assumed. A disrupted BBB that permits albumin transition into the CNS could further impact the course of MS given its ability to induce astrocyte and microglia activation, leading to an increased synthesis of glutamate or affecting potassium homeostasis, all potentially leading to functional and structural alterations of cortical circuits.²⁰ Hence, higher CSF_{Alb} might not only indicate BBB permeability alterations, but may also induce a further deleterious cascade for the long-term outcome of MS patients. Another IgA-dependent mechanism might be driven through meningeal mast cells that enhance via interleukin-6 the proliferation of B lymphocytes and induce their differentiation toward IgA-secreting plasma cells.²¹

In contrast to our results, a study by Uher et al.⁸ did not find any association between Q_{Alb} after the first clinical MS episode and the reduction of global normalized cortical volume (from 1.5T MRI) 48 months after disease onset. This discrepancy can be attributed to several factors. First, the assessment of global cortical volume is less sensitive to regional cortical reorganization processes. Moreover, the estimation of brain volumes depends on the MRI technical parameters (1.5T vs 3T) and the type of postprocessing algorithm used, since the segmentation-based algorithm FSL-SIENAX applied by Uher et al. shows more heterogeneous results in brain volume changes than the FreeSurfer-based analysis of CT²² adapted in our study.

Like Q_{Alb} and Q_{IgA}, Q_{IgG} was also associated with cortical atrophy rates, but showing fewer significant clusters. The pathogenic role of IgG in MS remains unclear, IgG OCB-positive MS patients having higher global and regional brain atrophy than IgG OCB-negative patients.²³ Rojas et al.²⁴ reported that the presence of

IgG OCB in CSF at MS onset is associated with the presence of brain volume reduction, mainly in neocortical GM regions, independent of lesion load and other clinical parameters. Due to the inclusion of a disproportionately large number of OCB-positive patients, analysis of the regional cortical differences depending on IgG OCB status was not possible.

Cortical remodeling is an important characteristic of evolving MS pathology mirroring the long-term progress of the disease.²⁵ We have recently shown gray matter network reorganization with a strengthening of local and modular cortical connectivity.¹ Divergent reorganization patterns of gray and white matter were associated with clinical impairment. Here, we detected cortical thinning in a regional pattern with maxima in the precuneus and parieto-occipital cortex. The precuneus is a central region for a large spectrum of neurocognitive functions, presenting a wide range of connections to middle frontal gyrus, amygdala, hippocampus, and thalamus.²⁶ The depicted structural alterations in these regions could be linked to emerging functional cognitive deficits in MS patients with conscious information processing or episodic memory alterations.

We did not find any correlation between CSF variables and the rate of thalamus atrophy. Since thalamic atrophy is detectable early in RRMS patients, a different and possibly BBB-albumin- and IgA-independent alteration of microstructural integrity can be postulated.²⁷

Conclusion

We determined that increased CSF concentrations of albumin, IgA, and IgM are associated with regional cortical atrophy and increased disability in patients with early MS and demonstrated a link between specific markers of immune response in the CSF, BBB function, and disease course.

Acknowledgements

J.K., D.C., F.Z., S.G.M., and S.G. contributed equally to this work. We thank Cheryl Ernest for proofreading the manuscript.

Declaration of Conflicting Interests

The author(s) declared no potential conflicts of interest with respect to the research, authorship, and/or publication of this article.

Funding

The author(s) disclosed receipt of the following financial support for the research, authorship, and/or publication of this article: This study has been supported by the German Research Foundation (DFG);

CRC-TR-128) and the Federal Ministry for Education and Research (BMBF; KKNMS).

References

1. Fleischer V, Gröger A, Koirala N, et al. Increased structural white and grey matter network connectivity compensates for functional decline in early multiple sclerosis. *Mult Scler* 2017; 23: 432–441.
2. Fleischer V, Kolb R, Groppa S, et al. Metabolic patterns in chronic multiple sclerosis lesions and normal-appearing white matter: Intraindividual comparison by using 2D MR spectroscopic imaging. *Radiology* 2016; 281: 536–543.
3. Jacobsen C, Hagemeyer J, Myhr K-M, et al. Brain atrophy and disability progression in multiple sclerosis patients: A 10-year follow-up study. *J Neurol Neurosurg Psychiatry* 2014; 85: 1109–1115.
4. Wiendl H and Meuth SG. Pharmacological approaches to delaying disability progression in patients with multiple sclerosis. *Drugs* 2015; 75: 947–977.
5. Lécuyer M-A, Saint-Laurent O, Bourbonnière L, et al. Dual role of ALCAM in neuroinflammation and blood-brain barrier homeostasis. *Proc Natl Acad Sci U S A* 2017; 114: E524–E533.
6. Kebir H, Ifergan I, Alvarez JI, et al. Preferential recruitment of interferon- γ -expressing TH17 cells in multiple sclerosis. *Ann Neurol* 2009; 66: 390–402.
7. Alvermann S, Hennig C, Stuve O, et al. Immunophenotyping of cerebrospinal fluid cells in multiple sclerosis: In search of biomarkers. *JAMA Neurol* 2014; 71: 905–912.
8. Uher T, Horakova D, Tyblova M, et al. Increased albumin quotient (QAlb) in patients after first clinical event suggestive of multiple sclerosis is associated with development of brain atrophy and greater disability 48 months later. *Mult Scler* 2016; 22: 770–781.
9. Polman CH, Reingold SC, Banwell B, et al. Diagnostic criteria for multiple sclerosis: 2010 revisions to the McDonald criteria. *Ann Neurol* 2011; 69: 292–302.
10. Droby A, Lukas C, Schänzer A, et al. A human post-mortem brain model for the standardization of multi-centre MRI studies. *Neuroimage* 2015; 110: 11–21.
11. Berlit P. *Klinische Neurologie*. Berlin: Springer, 2011.
12. Reiber H and Felgenhauer K. Protein transfer at the blood cerebrospinal fluid barrier and the quantitation of the humoral immune response within the central nervous system. *Clin Chim Acta* 1987; 163: 319–328.
13. Reiber H and Albaum W. Statistical evaluation of intrathecal protein synthesis in CSF/Serum quotient diagrams. *Acta Neuropsychiatr* 2008; 20: 47–48.
14. Schmidt P, Gaser C, Arsic M, et al. An automated tool for detection of FLAIR-hyperintense white-matter lesions in multiple sclerosis. *Neuroimage* 2012; 59: 3774–3783.
15. Reuter M, Rosas HD and Fischl B. Highly accurate inverse consistent registration: A robust approach. *Neuroimage* 2010; 53: 1181–1196.
16. Hanganu A, Groppa SA, Deuschl G, et al. Cortical thickness changes associated with photoparoxysmal response. *Brain Topogr* 2015; 28: 702–709.
17. Reuter M, Schmansky NJ, Rosas HD, et al. Within-subject template estimation for unbiased longitudinal image analysis. *Neuroimage* 2012; 61: 1402–1418.
18. Lucchinetti CF, Popescu BF, Bunyan RF, et al. Inflammatory cortical demyelination in early multiple sclerosis. *N Engl J Med* 2011; 365: 2188–2197.
19. Freedman MS, Thompson EJ, Deisenhammer F, et al. Recommended standard of cerebrospinal fluid analysis in the diagnosis of multiple sclerosis: A consensus statement. *Arch Neurol* 2005; 62: 865–870.
20. LeVine SM. Albumin and multiple sclerosis. *BMC Neurol* 2016; 16: 47.
21. Merluzzi S, Frossi B, Gri G, et al. Mast cells enhance proliferation of B lymphocytes and drive their differentiation toward IgA-secreting plasma cells. *Blood* 2010; 115: 2810–2817.
22. Durand-Dubief F, Belaroussi B, Armspach J, et al. Reliability of longitudinal brain volume loss measurements between 2 sites in patients with multiple sclerosis: Comparison of 7 quantification techniques. *Am J Neuroradiol* 2012; 33: 1918–1924.
23. Ferreira D, Voevodskaya O, Imrell K, et al. Multiple sclerosis patients lacking oligoclonal bands in the cerebrospinal fluid have less global and regional brain atrophy. *J Neuroimmunol* 2014; 274: 149–154.
24. Rojas JI, Patrucco L, Tizio S, et al. Oligoclonal bands in the cerebrospinal fluid and increased brain atrophy in early stages of relapsing-remitting multiple sclerosis. *Arq Neuropsiquiatria* 2012; 70: 574–577.
25. Calabrese M, Rinaldi F, Mattisi I, et al. Widespread cortical thinning characterizes patients with MS with mild cognitive impairment. *Neurology* 2010; 74: 321–328.
26. Cavanna AE and Trimble MR. The precuneus: A review of its functional anatomy and behavioural correlates. *Brain* 2006; 129: 564–583.
27. Deppe M, Krämer J, Tenberge JG, et al. Early silent microstructural degeneration and atrophy of the thalamocortical network in multiple sclerosis. *Hum Brain Mapp* 2016; 37: 1866–1879.